

An investigation on frost resistance and pore structure of alkali-activated slag concrete

Xiaomei Wan^{1,2*}, Chen Shen¹, Penggang Wang^{1,2}, Tiejun Zhao^{1,2}, Shuwen Zhang¹, Yu Lu¹

¹ School of Civil Engineering, Qingdao University of Technology, Qingdao, China

² Cooperative Innovation Center of Engineering Construction and Safety in Shandong Blue Economic Zone, Qingdao University of Technology, Qingdao, China.

*corresponding author; Xiaomei Wan

ABSTRACT: Alkali-activated cementitious materials possess advantages such as sustainability and waste-recycling potential and they may have great development in the future. In this paper, the freeze-thaw resistance of alkali-activated slag concretes with different mix proportion are researched experimentally. The effects of alkaline activator types and blend of fly ash on mechanical properties and frost resistance of alkali-activated slag concrete is studied respectively. Compared with specimen of slag activated by NaOH, the one of slag activated by water glass attain higher strength and frost resistance. The morphology and pore structure of alkali-activated slag concrete were analyzed by mercury intrusion test, nitrogen adsorption test and scanning electron microscope. The results are in relatively reasonable agreement with the model of physical damage degree and freeze-thaw cycles. The pore size range of samples of slag activated by water glass is almost below 30 nm, and the change of pore structure after freeze-thaw cycles is minor. However, the pore size range of the samples of slag activated by NaOH is mainly within 50 nm, while the pore structure changes significantly and the pore size increases obviously after freeze-thaw cycles.

Keywords: alkali-activated slag concrete; frost resistance; pore structure; morphology.

Date of Submission: 05-09-2019

Date of acceptance: 22-09-2019

List of notations

E_r is the relative dynamic elastic modulus of concrete

W_1 is the mass loss rate

N is the number of freeze-thaw cycles

ω is the damage degree

a, b, c and d represent material characteristic parameters determined by experiments

e, f is the fitting parameters

I. INTRODUCTION

Frost damage is a primary reason for the reduction of performance of concrete structure in cold regions. Ice crystal expansion from frost leads to cracking, scaling, loss in mechanical properties, and eventually the destruction of concrete structure. The mechanism of frost damage of cementitious concrete has been extensively studied (Wakimoto K et al., 2008; Powers TC, 1949; Powers TC and Helmuth RA, 1953; Coussy O and Monteiro PJM, 2008; Çopuroğlu O and Schlangen E, 2008; Coussy O and Monteiro PJM, 2009; Beaudoin JJ and Macinnis C, 1974; Coussy O, 2005). Since the 1930s, the strong theoretical basis is provided for the freeze-resistant design of structures (Scherer GW and Valenza JJ, 2005; Powers TC, 1965). The segregation stratification hypothesis put forward by Collins (1994) holds that the frost damage of concrete is due to the freezing of pore water at different depths in concrete members at low temperatures. The model of concrete frost damage proposed by Powers (1945). Powers and Helmuth (1953) projected the osmotic pressure hypothesis that the pore solution contains K^+ , Ca^{2+} , Na^+ and some of the solutions in the larger pore are frozen first, while the remaining solution ion concentration rises, and the pore solution connected with it has a lower concentration.

Therefore, water will flow to the unfrozen macropore under the action of osmotic pressure. Fagerlund (1979) raised the theory of critical water saturation. Subsequently, more scholars enriched and perfected previous theories and put forward a series of new theories (Mihta PK et al., 1992; Setzer MJ, 2001; Penttala V, 2006). However, there is still a numbers of researches on frost damage mechanisms of alkali-activated slag concrete, AASC (Palomo A et al., 1999; Ferández-Jiménez A et al., 1999; Bakharev T et al., 2000), which is normally prepared from industrial waste or by-products (such as kaolinite ore, slag or fly ash) containing pozzolanic effect and chemical activator. AASC is used more and more widely and expected to replace cement in some situations because of high strength, durability and sustainability.

In this study, the deterioration characteristic of alkali-activated slag concrete subjected to cyclic freeze-thaw attacks are evaluated. The quantification criteria based on the strength before and after freeze-thaw cycles, relative dynamic elastic modulus (RDEM), mass loss (ML) are calculated. The physical damage degree of specimens after freeze-thaw cycles are evaluated based on results and fitting models. Furthermore, the morphology of the samples is analyzed by microscopic tests (SEM); the pore structure is analyzed by mercury intrusion test (MIP) and nitrogen adsorption test.

II. MATERIALS AND METHODS

2.1. Materials and mix proportions of specimens

A granulated blast furnace slag with specific surface of 523 m²/kg and a class II fly ash were selected in this study. The chemical compositions of GBFS and FA as precursor binding materials are given in Table 1. NaOH solution or NaOH/water glass mixed solution was used as alkaline activator, the modulus of NaOH/water glass was adjusted to 1.8 and 2.0. Aggregates consist of local river sand with a maximum grain size of 5 mm and crushed basalt with a maximum size of 20 mm.

Table 1. Chemical composition of granulated blast furnace slag and fly ash.

% wt	CaO	SiO ₂	Al ₂ O ₃	MgO	Fe ₂ O ₃	SO ₃	Na ₂ O	K ₂ O	MnO	BaO	P ₂ O ₅	TiO ₂
BFS	41.6	26.81	17.79	9.28	0.48	2.03	0.31	0.39	0.34	0.09	0.02	0.72
FA	5.79	66.8	17.93	1.5	4.03	0.5	0.26	1.32	0.06	0.08	0.43	1.07

Seven mixes of alkali-activated slag and fly-ash concrete are listed in Table 2. After being mixed, fresh concrete was poured into prismatic molds with dimensions of 100 mm× 100 mm× 400 mm for freeze-thaw cycle test and corresponding mechanical properties test. A 100mm cubic concretes were fabricated for the compressive strength test. After 24 h, the specimens were demoulded and cured under a relative humidity of 95 % and a temperature of 20 ± 3 °C until the age of test. Compressive strength was tested on cubic specimens according to the testing procedures specified in GB/T 50081-2002 at the age of 7, 14 and 28 curing days.

Table 2. Mix proportion of AASC specimens.

Mix. Group	Activator	Na ₂ O Alkaline solution, wt. %	in Solution, kg/m ³	Coarse Aggregate, kg/m ³	Sand, kg/m ³	Slag, kg/m ³	Fly Ash, kg/m ³
1	NaOH	7	184	1074	716	400	0
2	NaOH	9	184	1074	716	400	0
3	NaOH	9	184	1074	716	320	80
4	water glass (M=1.8)	7	184	1074	716	400	0
5	water glass (M=1.8)	9	184	1074	716	400	0
6	water glass (M=1.8)	9	184	1074	716	320	80
7	water glass (M=2.0)	9	184	1074	716	400	0

2.2. Freeze-thaw cycles test

Cyclic freeze-thaw tests were conducted to determine the frost resistance of alkali-activated slag concrete referring to the Chinese specification GB/T 50082-2009. Three specimens in each group for freeze-thaw cycle test. The specimens were subjected to 300 freeze-thaw cycles at most and relative dynamic elastic modulus (RDEM) and mass loss (ML) were measured every 25 cycles. Each freeze-thaw cycle takes two hours, freezing for 1.5 hours and thawing for 0.5 hours. The dynamic elastic modulus of alkali-activated slag concrete was measured by resonance dynamic elastic modulus tester, while the mass of the specimen was

weighed.

2.3. Calculation of frost damage

The frost deterioration model of concrete is related to the damage mechanics, and there are many damage indexes of ordinary concrete structure, including accumulative frost damage, relative dynamic elastic modulus attenuation, strength attenuation, damage degree, mass attenuation and so on. In this paper, the damage degree is taken as the damage index of alkali-activated slag concrete under frost environment, and the damage degree model was fitted.

Mu (2000) revised the logarithmic law of Ghafoori and got a model which can reflect the law of mass loss of concrete blocks in different frost stages (Eq. 1). And the damage degree ω is defined as Eq. 2:

$$W_1 = a \cdot \lg(bN + 1) \left(1 + c \frac{10^{(0.01N-d)}}{1+10^{(0.01N-d)}} \right) \quad (1)$$

$$\omega = 1 \pm \frac{0.05 - W_1}{0.05} \times \frac{E_r - 0.6}{0.4} \quad (2)$$

where E_r is the relative dynamic elastic modulus of concrete, W_1 is the mass loss rate. N is the number of freeze-thaw cycles, a , b , c and d represent material characteristic parameters determined by experiments.

According to damage mechanics, Liu et al. (2005) obtained the mathematical model of damage degree and freeze-thaw cycle number, as follows:

$$\omega = e \cdot N^f \quad (3)$$

where e and f are fitting parameters, N is the number of freeze/thaw cycles.

2.4. Microstructure test

The morphology and element analysis of concretes were analyzed by Scanning Electron Microscopy and Energy Dispersive Spectrometer (SEM-EDS), conducted on an EVO MA18 40XVP instrument at 25 kV. The porous structure was studied by mercury intrusion porosimetry (MIP) and nitrogen adsorption. Mercury intrusion porosimetry was carried out on Auto Pore IV High-Performance Automatic Mercury Injection Instrument and nitrogen adsorption test was conducted on the AutoChem II 2920 Chemical Adsorbent Instrument.

III. RESULTS AND DISCUSSION

3.1. Mechanical and physical properties

The results of 100mm cube compressive strength of each mix are illustrated in figure 1. Fly ash particles are spherical and have ball effect to lubricate, which can improve the fluidity of concrete (Niu JS and Ma XW, 2011). However, the Si-rich phase and Al-rich phase in fly ash glass beads are difficult to release, resulting in a low degree of hydration reaction, which is not conducive to the development of concrete strength (Mix 3 and Mix 6). Compressive strength of AASC specimens activated by water glass is significantly higher than that of AAS specimens activated by NaOH solution. And the specimens activated by alkali with higher Na_2O % yield higher compressive strength. It can be also found that water glass with higher modulus contributes to the improvement of the compressive strength of AASC.

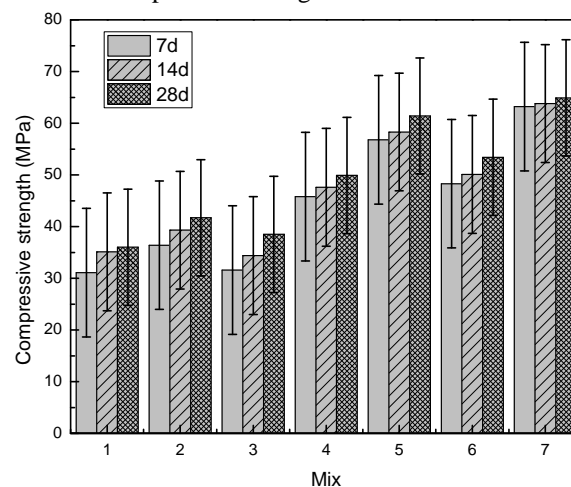


Fig. 1 Compressive strength of AASC.

The appearance of AASC specimens after 300 freeze-thaw cycles are shown in figure 2. The surface of the specimens with NaOH solution as activator is severely scaled, while the ones with water glass as activator has no obvious defect after the same freeze-thaw cycles. With the increase of freeze-thaw cycle times, relative dynamic elasticity modulus of specimens with water glass as activator decreases in varying degrees relatively slowly (as shown in figure 3). Compared with Mix 7 which keeps the relative dynamic elasticity modulus of 96% even after 300 freeze-thaw cycles, the relative dynamic modulus of specimens with NaOH as activator decreases by nearly 50%. As seen in figure 4, the mass loss of NaOH-activated specimens is more than 5% when the fast freeze-thaw cycle is less than 175 cycles. By contrast, for the specimens with water glass as activator and without fly ash, the mass loss is still very low after 300 cycles.



Fig. 2 Appearance of AASC specimens after 300 freeze-thaw cycles. (a) Specimens with NaOH as activator;(b) Specimens with water glass as activator.

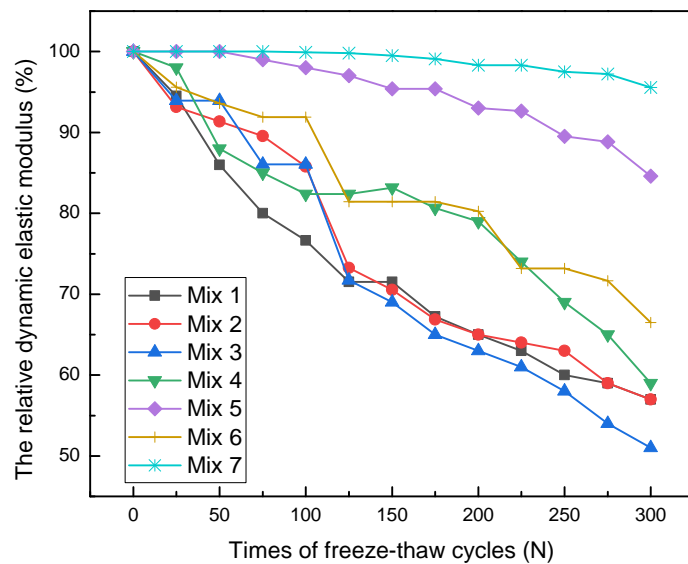


Fig. 3 Variation of relative dynamic elasticity modulus with times of freeze–thaw cycles.

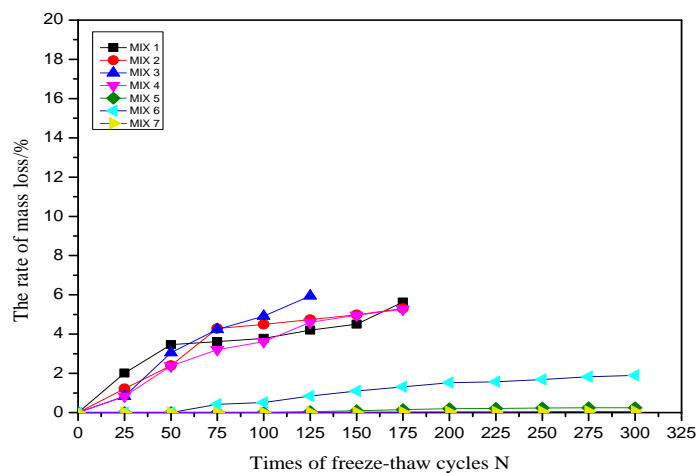


Fig. 4 Variation of mass loss with freeze–thaw cycles.

According to Standard for Test Methods of Long-Term Performance and Durability of Ordinary Concrete (GB/T 50082- 2009), if relative dynamic elastic modulus is less than 60% or weight loss is more than 5%, the specimens is thought damaged. The relationship between maximum number of freeze-thaw cycles and compressive strength of AASC is summarized in figure 5. It is shown that the 100mm cube strength of specimens is closely correlated with frost resistance.

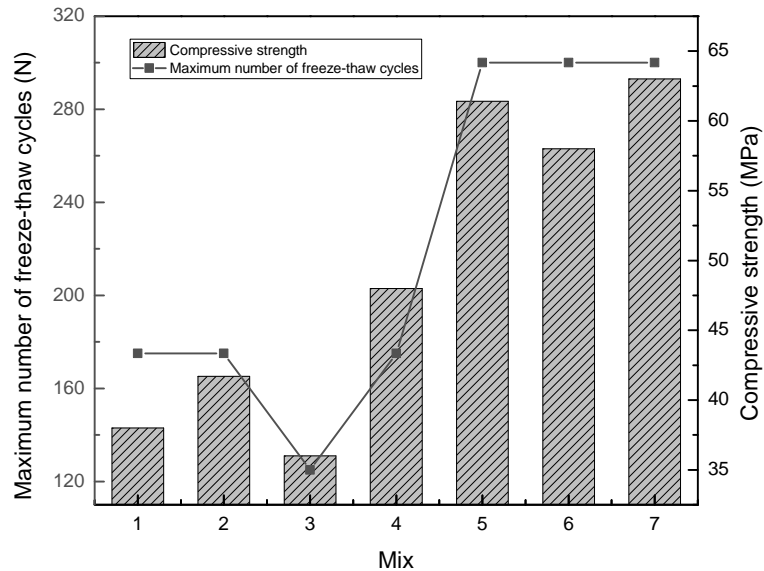


Fig. 5 Relationship between 28d compressive strength and maximum number of freeze-thaw cycles.

3.2. Frost damage

The damage degree from experimental data is fitted according to Eq. 3 as shown in figure 6. The relationships between damage degree and freeze-thaw cycles of alkali-activated slag concrete and ordinary Portland concrete with the same strength grade are shown in figure 7. The results show that the frost damage degree of water glass activated samples after 300 freeze-thaw cycles is the lowest. By contrast, frost damage degree of NaOH solution activated samples is the highest, which reaches 0.98 after 125 cycles. Compared with the same strength grade of OPC, the damage degree of AASC activated by water glass is relatively low especially before 200 freeze-thaw cycles, while that of AASC activated by NaOH is higher. Although they are not specifically designed for frost resistance, the frost resistance of ASC stimulated by sodium silicate meets the requirements of frost-resistant concrete.

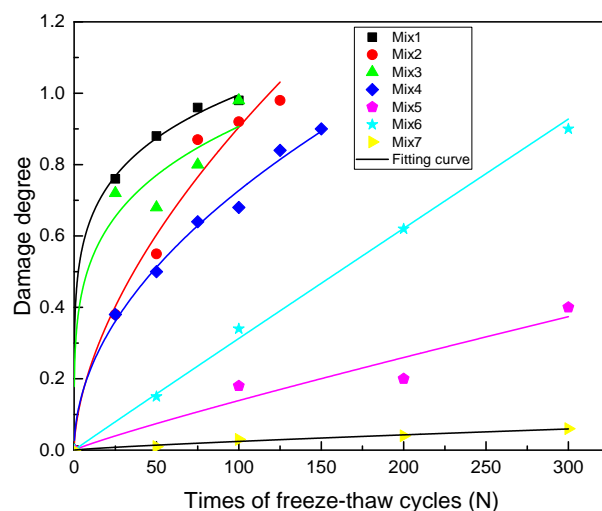


Fig.6. Deterioration model of frost damage.

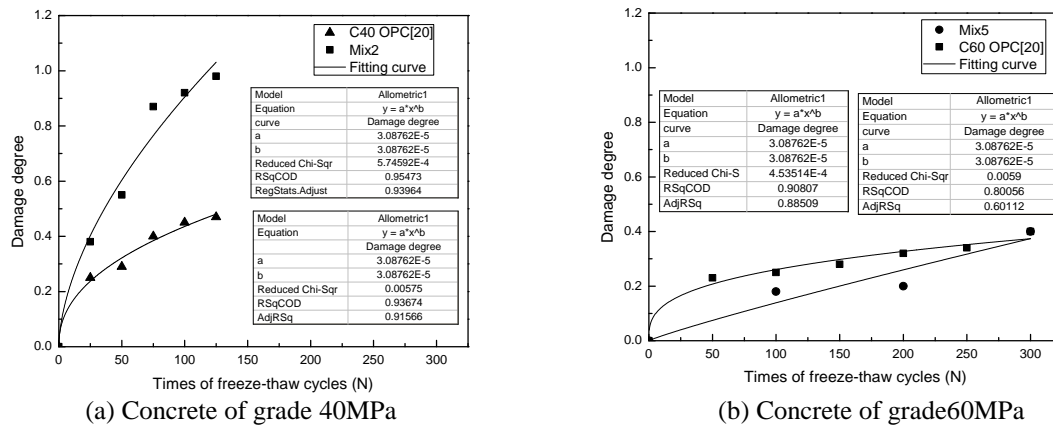


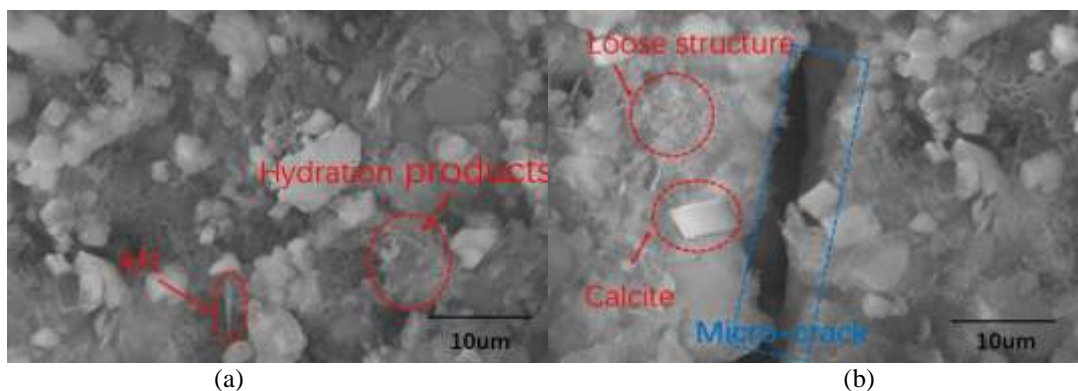
Fig. 7 Relationship between frost damage and freeze-thaw cycles.

3.3. Morphology and pore structure

3.3.1. Morphology

Scanning electron microscope images of Mix 2, Mix 5 and Mix 6 before and after freeze-thaw cycles are presented in figure 8. Energy dispersive spectrometer (EDS) analysis of hydration products of Mix 6 was carried out and the results are provided in figure 9. Even though larger cracks can be observed, the entire structure of samples activated by water glass is found more uniform and compacted, in which there is no obvious interface transition zone. With the addition of fly ash, there are some micro-cracks in the sample under SEM. Some studies have shown that the micro-cracks may be caused by the different chemical shrinkage of the hydration products of alkali slag (C-(A)-S-H) and the hydration products of alkali fly ash (N-A-S-H) (Puertas F et al., 2000). By contrast, no obvious cracks are found in NaOH-activated slag samples, but more flocculent, needle-bar, and partially unhydrated particles exist in the samples. After 300 freeze-thaw cycles, each sample has been damaged to various degrees. However, samples activated by water glass have better integrity and therefore higher frost resistance though a few cracks exist.

Generally, the morphology of samples of AAS are even and close-grained, cemented with surrounding binding products, in which there is no coarse crystal of $Ca(OH)_2$, thus frost resistance of AAS was improved. Lee and Van Deventer (2004) founded that there is no obvious interface transition zone in alkali-activated materials with water glass as activator, which can be confirmed in the experiment in this paper. EDS results show that O, Si, Ca, Al, Mg, and Na are the main elements in hydration products of AAS. The main hydration product is C-A-S-H with low calcium-silicon ratio. Wang et al. (1995) stated that the presence of Al atoms contributes to the polymerization of the silicate tetrahedron and transform the short chains to the branching morphology of C-A-S-H gel. Close-grained hydration products and absence of interfacial transition zone of alkali-activated slag lead to denser microstructure and higher frost resistance.



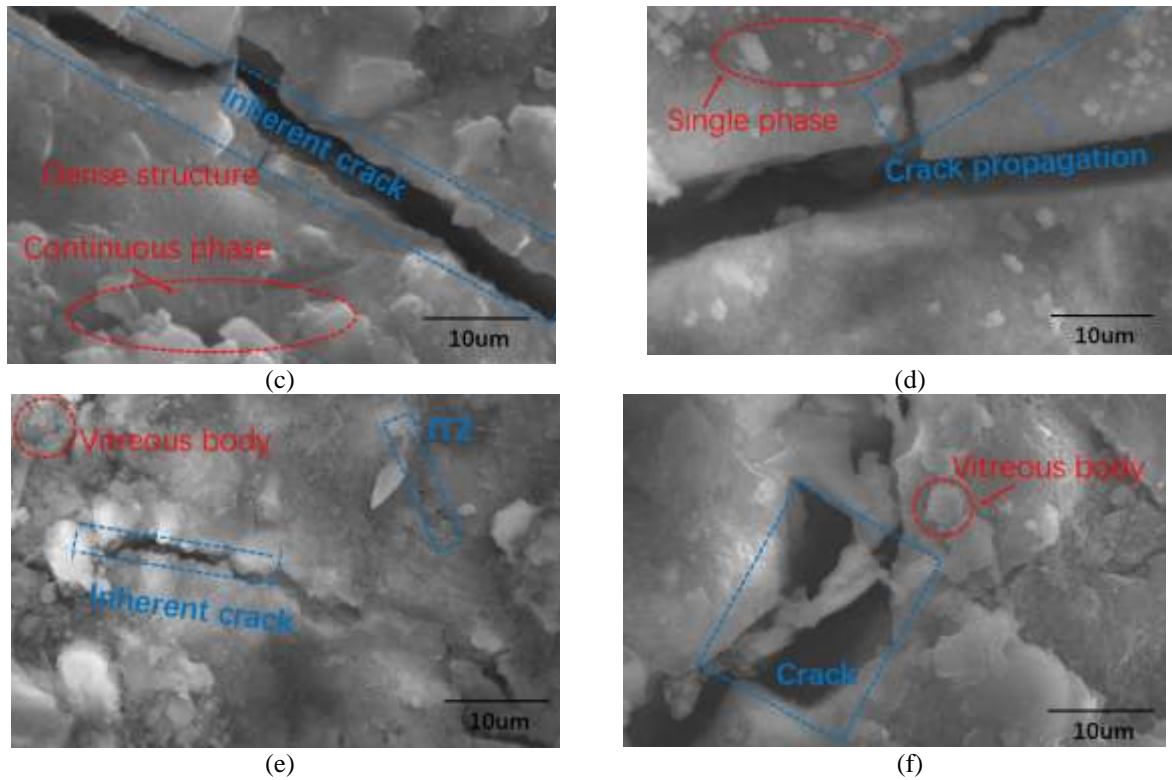
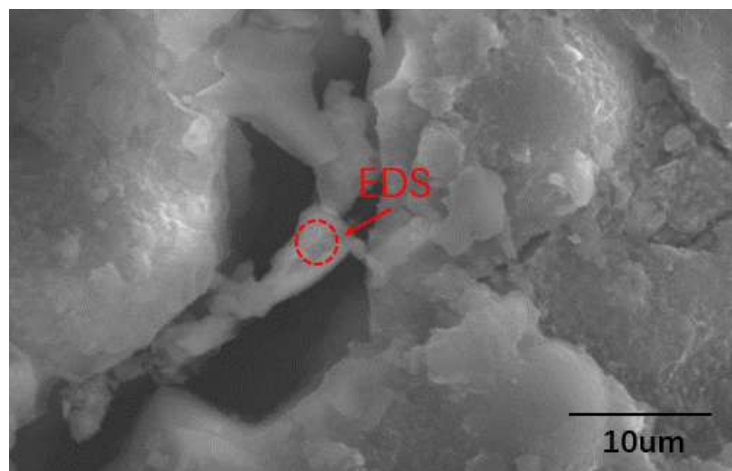
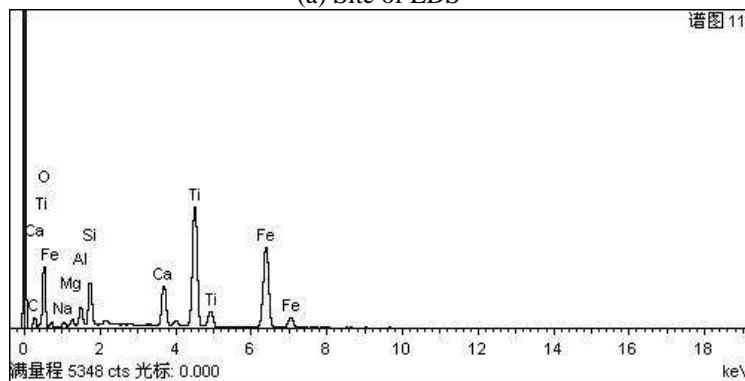


Fig.8 SEM analysis before and after freeze-thaw cycles. (a) Mix 2 before freeze-thaw cycles; (b) Mix 2 after freeze-thaw cycles; (c) Mix 5 before freeze-thaw cycles; (d) Mix 5 after freeze-thaw cycles; (e) Mix 6 before freeze-thaw cycles of; (f) Mix 6 after freeze-thaw cycles.



(a) Site of EDS



(b)EDS Spectrum

Fig.9. SEM-EDS of Mix 6

3.3.2 Pore structure

The pore structure of samples of AAS (Mix 2, Mix 5, Mix 6) is analyzed by mercury intrusion method and nitrogen adsorption method respectively. From the pore size distribution curves of MIP results presented in figure 10, the findings can be summarized as follows: The pore diameters of AAS samples are less than 100 nm generally and mainly concentrated in the range of 10-30 nm; After freeze-thaw cycles, the pore size of the samples activated by water glass changes slightly compared with that before freeze-thaw cycles (Mix5 and Mix6), while the pore volume of the samples activated by NaOH increases significantly (Mix 2). Combined with the results of scanning electron microscopy, samples activated by water glass behave higher frost resistance compared with that activated by NaOH.

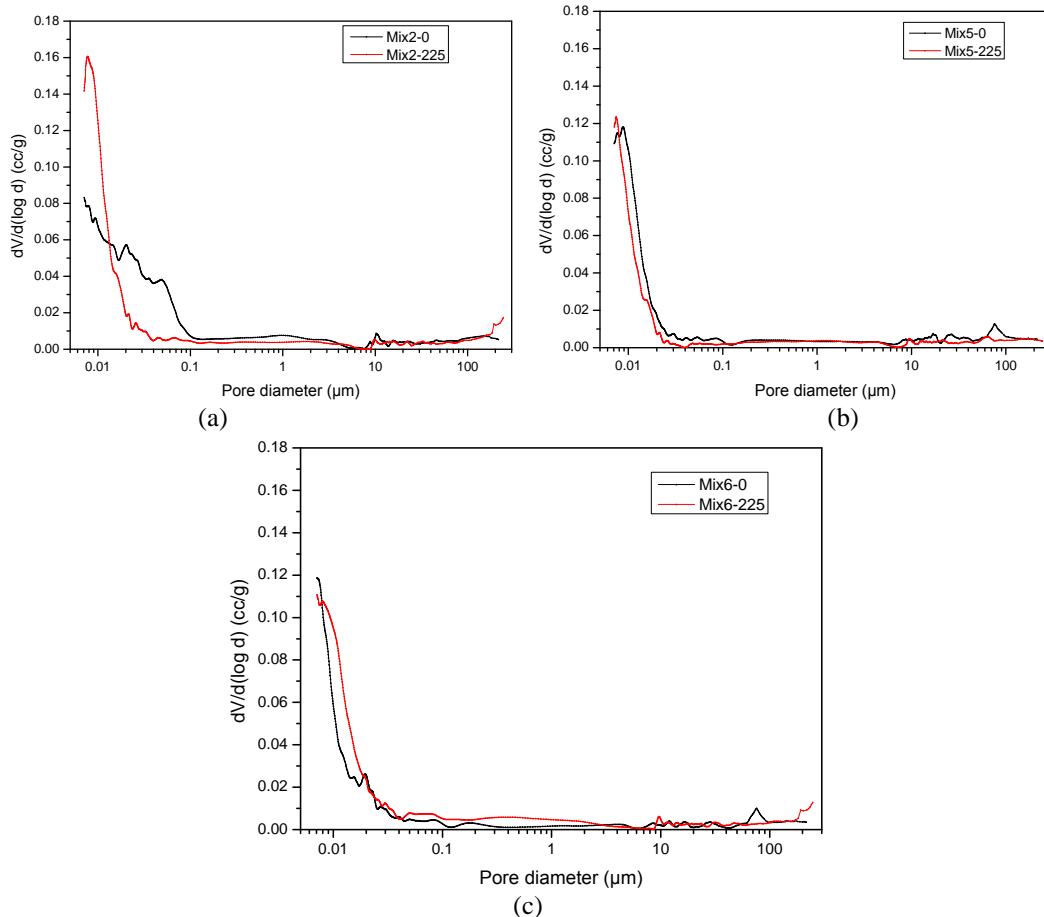


Fig.10. Pore size distribution curve measured by MIP. (a) Pore size distribution of Mix 2; (b) Pore size distribution of Mix 5; (c) Pore size distribution of Mix 6.

For obtain the pore size distribution in the range of 2-100 nm, nitrogen sorption porosimetry was applied and the measured curves are shown in figure 11. For samples activated by water glass (Mix5 and Mix6), the main pore size is less than 60 nm, and the pore size range increases slightly with the addition of fly ash. For samples activated by NaOH (Mix2), the pore size is distributed beyond 110 nm mainly and has a wider range. After rapid freeze-thaw cycles, the pore structure of samples activated by NaOH changes obviously, and the pore size and volume increase enormously.

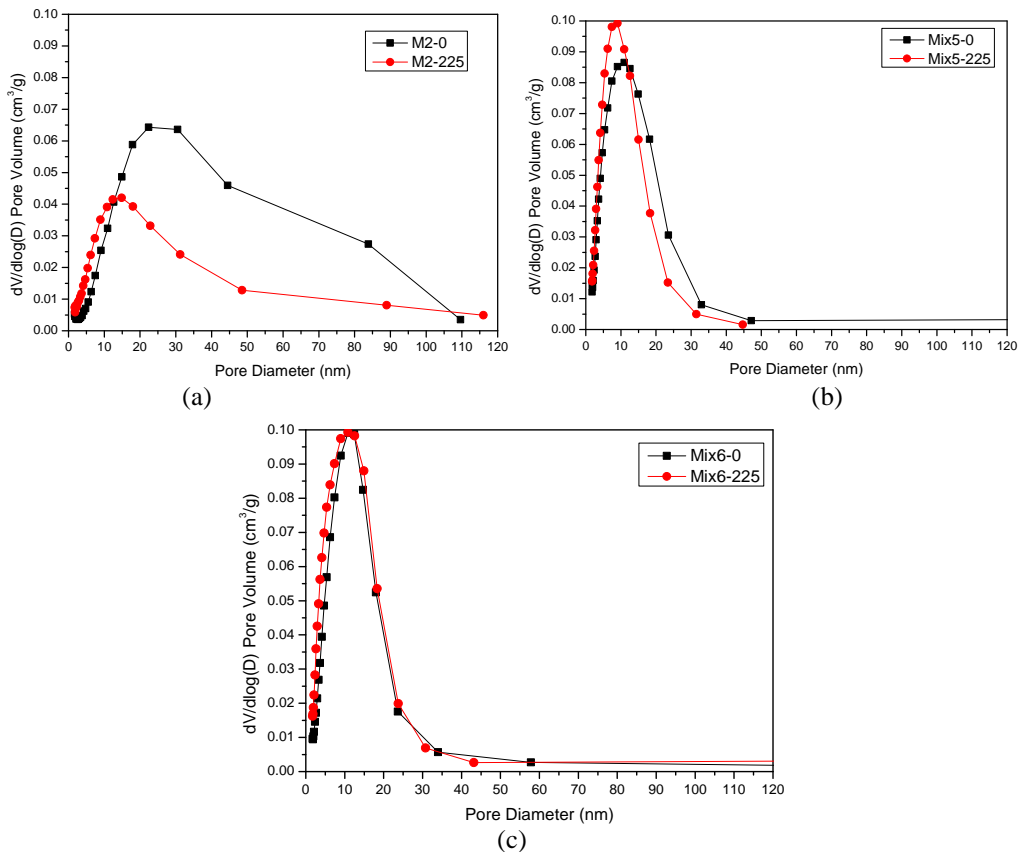
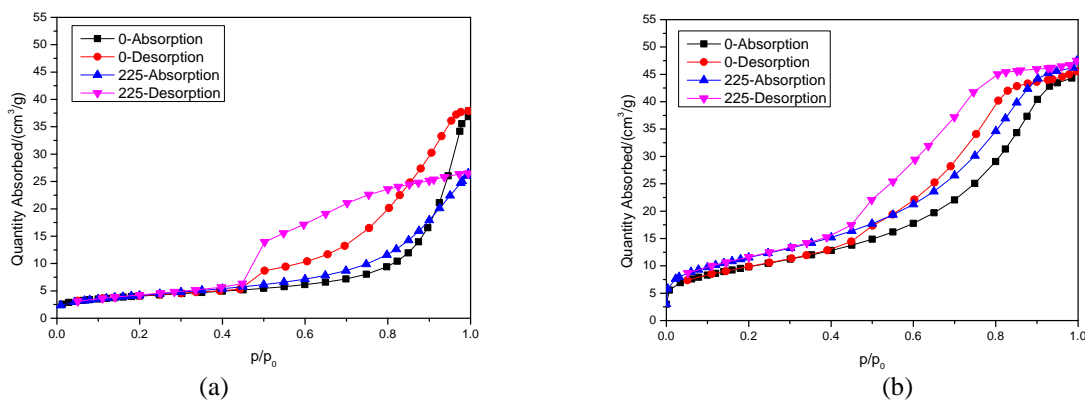


Fig. 11. Pore size distribution curve measured by nitrogen adsorption. (a) Pore size distribution of Mix 2; (b) Pore size distribution of Mix 5; (c) Pore size distribution of Mix 6.

Figure 12 presents the nitrogen adsorption and desorption curve of alkali-activated slag concrete before and after 225 freeze-thaw cycles. Figure 13 illustrates the six types of physical adsorption isotherm classified by the International Union of Pure and Applied Chemistry (IUPAC) (International Union of Pure and Applied Chemistry Physical Chemistry Division Commission on Colloid and Surface Chemistry, 1994).

By comparing with figure 13, it can be concluded that the adsorption isotherms of slag activated by NaOH belongs to type I, which presents mesoporous material with relatively narrow pore size distribution (Sun FL, 2015; Sing KSW et al.,1985). The adsorption isotherms of samples after 225 freeze-thaw cycles belong to type II, and the pore size distribution is wider than that before freeze-thaw cycles. Both the pore size distribution of the slag activated by water glass before and after freeze-thaw cycles belong to type I. The adsorption-desorption curve indicates that the specific surface area of the frost sample increase, while there is no essential change in the pore size distribution characteristics. The pore volume of samples blended with fly ash increased obviously after freeze-thaw cycles compared with that of samples without fly ash.



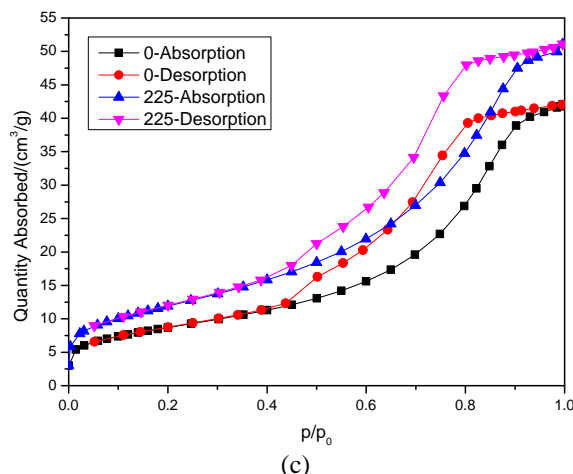


Fig. 12. Nitrogen adsorption and desorption curves of AASC. (a) Mix 2; (b) Mix 5; (c) Mix 6.

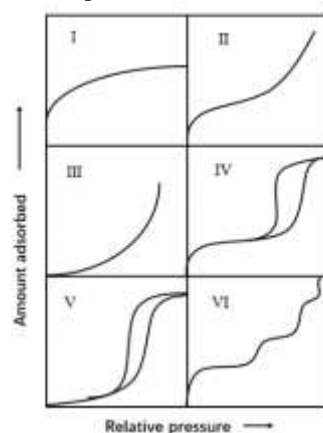


Fig. 13. Types of adsorption isotherms [[28]].

IV. CONCLUSION

The compressive strength and relative dynamic elastic modulus of alkali-activated slag concrete specimens with water glass as activator after freeze-thaw cycles are significantly higher than that of alkali-activated slag concrete specimens with NaOH solutions as activator, while the mass loss rate after freeze-thaw cycles of former is lower than the latter. Higher Na₂O content of alkaline activator and higher modulus of water glass also contribute to the frost resistant of AASC specimens. Furthermore, the blend of fly ash is not benefit to the compressive strength and frost resistance of AASC. The results are in reasonable agreement with the model of physical damage degree and freeze-thaw cycles.

The pore size of the slag sample activated by water glass are basically distributed in the range below 30 nm, and the change of pore structure is minor after freeze-thaw cycles. By contrast, the pore size of the specimens activated by NaOH solutions is mainly within 50 nm, and the pore size increases and pore structure changes significantly after freeze-thaw cycles. The nitrogen adsorption and desorption analysis concluded that slag activated by NaOH shows that the sample is mainly mesoporous material with a relatively narrow pore size distribution, and the pore size distribution tends to wider after freeze-thaw cycles. There is no obvious change in the pore size distribution of the slag sample activated by water glass before and after freeze-thaw cycles.

ACKNOWLEDGEMENTS

This research was funded by National Natural Science Foundation of China (grant number 51878365), key project of international cooperation from National Natural Science Foundation of China (grant number 51420105015) and Natural Science Foundation of Shandong Province (grant number ZR2017MEE040).

REFERENCES

- [1]. Wakimoto K, Blunt J, Carlos C et al. (2008) Digital laminography assessment of the damage in concrete exposed to freezing temperatures. *Cement and Concrete Research* 38(10): 1232-1245.
- [2]. Powers TC. (1949) The air requirement of frost-resistant concrete. *Highway Research Board Proceedings* 33(29): 184-211.
- [3]. Powers TC, Helmuth RA. (1953) Theory of volume changes in hardened Portland cement paste during freezing. *Highway Research Board Proceedings* 32: 286-297.

- [4]. Coussy O, Monteiro PJM. (2008) Poroelastic model for concrete exposed to freezing temperatures. *Cement and Concrete Research* 38(1): 40-48.
- [5]. Çopuroğlu O, Schlangen E. (2008) Modeling of frost salt scaling. *Cement and Concrete Research* 38(1): 27-39.
- [6]. Coussy O, Monteiro PJM. (2009) Errata to "Poroelastic model for concrete exposed to freezing temperatures" *Cement and Concrete Research* 39(4): 371-372.
- [7]. Beaudoin JJ, Macinnis C. (1974) The mechanism of frost damage in hardened cement paste. *Cement and Concrete Research* 4(2): 139-147.
- [8]. Coussy O. (2005) Poromechanics of freezing materials. *Journal of the Mechanics and Physics of Solids* 53(8): 1689-1718.
- [9]. Scherer GW, Valenza JJ. (2005) Mechanism of Frost Damage to Concrete. In *Materials Science of Concrete VII*(Young F, Skalny J (ed.)). American Ceramic Society. US.
- [10]. Powers TC. (1965) The mechanisms of frost action in concrete. Stanton Walker Lecture Series on the Material Science, Lecture No.3. University of Maryland. Maryland, US.
- [11]. Clifton AR. (1944) The destruction of concrete by frost. *Journal of the Institution of Civil Engineers* 23(1): 29-41.
- [12]. Powers TC. (1945) A working hypothesis for further studies of frost resistance of concrete. *Journal of the American Concrete Institute* 16(4): 245-272.
- [13]. Fagerlund G. (1979) Prediction of the service life of concrete exposed to frost action. Study on concrete technology. Stockholm: Swedish Cement and Concrete Research Institute.
- [14]. Mihta PK, Schiessl P, Raupaeh M. (1992) Performance and durability of concrete systems. In *Proceedings of 5th international congress on the chemistry cement*. Vol. 1, pp. 571-659.
- [15]. Setzer MJ. (2001) Micro-ice-lens formation in porous solid. *Journal of Colloid and Interface Science* 243(1): 193-201.
- [16]. Penttala V. (2006) Surface and internal deterioration of concrete due to saline and non-saline freeze-thaw loads. *Cement and Concrete Research* 36(5): 921-928.
- [17]. Palomo A, Grutzeck MW, Blanco MT. (1999) Alkali-activated fly ashes: a cement for the future. *Cement and Concrete Research* 29(8): 1323-1329.
- [18]. Fernández-Jiménez A, Palomo A, Puertas F et al. (1999) Alkali-activated slag mortars mechanical strength behavior. *Cement and Concrete Research* 29(8): 1313-1321.
- [19]. Bakharev T, Sanjayan JG, Cheng YB. (2000) Effect of admixtures on properties of alkali activated slag concrete. *Cement and Concrete Research* 30(9): 1367-1374.
- [20]. Mu R. (2000) Durability and life prediction of concrete under combined action of freeze-thaw cycle and external bending stress and salt solution. Southeast University. (in Chinese)
- [21]. Liu ZY, Ma LG. (2005) Frost resistance and life prediction model of high strength concrete. *Industrial Construction* 35(1): 11-14. (in Chinese)
- [22]. Niu JS, Ma XW. (2011) Effect of Fly Ash on the Workability of Non-dispersible Underwater Concrete. *Advanced Materials Research* 194-196: 942-946.
- [23]. Puertas F, Martínez-Ramírez S, Alonso S et al. (2000) Alkali-activated fly ash/slag cements: Strength behavior and hydration products. *Cement and Concrete Research* 30(10): 1625-1632.
- [24]. Lee WKW, Deventer V. (2004) The interface between natural siliceous aggregates and geopolymers. *Cement and Concrete Research* 34(2): 195-206.
- [25]. Wang SD, Scrivener KL. (1995) Hydration products of alkali activated slag cement. *Cement and Concrete Research* 25(3): 561-571.
- [26]. International Union of Pure and Applied Chemistry Physical Chemistry Division Commission on Colloid and Surface Chemistry, Subcommittee on Characterization of Porous Solids. (1994) "Recommendations for the characterization of porous solids (Technical Report)", *Pure and Applied Chemistry* 66(8): 1739-1758.
- [27]. Sun FL. (2015) Study on the relationship between parameters of adsorption equilibrium model and temperature. Nanjing University of Technology. (in Chinese)
- [28]. Sing KSW, Everett DH, Haul RAW et al. (1985) Reporting physisorption data for gas solid systems with special reference to the determination of surface-area and porosity. *Pure and Applied Chemistry* 57(4): 603-619.

Karim, F.R." The influence of the brittleness index on fibrous normal strength concrete beams under pure torsion" *American Journal of Engineering Research (AJER)*, vol. 8, no. 9, 2019, pp 120-130